scientific reports

Check for updates

OPEN

Exploring the potential mechanism of B-phycoerythrin on DSS-induced colitis and colitis-associated bone loss based on network pharmacology, molecular docking, and experimental validation

Luming Deng[1,2,4,5], Zhenhui Feng[1,2,5], Xingyan Li[1,2,5], Lvhua Fan[1], Xia Wu[1,2], Samad Tavakoli[1], Yuzhen Zhu[1,2], Hua Ye[2,3,4]✉ & Kefeng Wu[1,2,3,4]✉

B-phycoerythrin (B-PE), a pigment protein, has found extensive applications in the food, pharmaceutical, and cosmetic industries. However, the effects and potential mechanisms of B-PE on colitis and colitis-associated bone loss remain unclear. Thus, the aim of this study was to investigate the pharmacological mechanisms of B-PE against colitis and colitis-associated bone loss using network pharmacology analysis, molecular docking, and experimental validation. Based on public databases, 99 common targets of B-PE against inflammatory bowel disease and osteoporosis were predicted. The protein-protein interaction network identified 16 core targets, including TNF, AKT1, EGFR, etc., as hub targets. Additionally, functional enrichment analyses and molecular docking results revealed that the PI3K/AKT signaling pathway may serve as a potential signaling pathway for B-PE in the treatment of colitis and colitis-associated bone loss. Furthermore, pharmacological experiments indicated that B-PE not only reversed the elevated expression of TNF-α, IL-1β, MMP9, and CXCL8a, and the reduced expression of ZO-1, E-cadherin, COL1A1, and RUNX2 in the DSS-induced colitis zebrafish model, but also enhanced the phosphorylation of PI3K and AKT, thereby mitigating inflammatory response and promoting osteogenesis. In conclusion, this study provides a theoretical basis for considering B-PE as a promising candidate for the treatment of colitis and colitis-associated bone loss.

Keywords B-phycoerythrin, Inflammatory bowel disease, Osteoporosis, Network pharmacology, Molecular docking, PI3K/AKT signaling pathway

Inflammatory bowel disease (IBD), which encompasses Crohn's disease (CD) and ulcerative colitis (UC), is a chronic, relapsing, and intractable inflammatory condition of the gastrointestinal tract. It is characterized by symptoms such as abdominal pain, diarrhea, bloody stool, fatigue, and weight loss[1,2]. In recent years, the incidence of IBD has not only remained high in the United States and Europe but has also rapidly increased in developing countries, including those in Asia and Africa[3]. Recurrent and prolonged illnesses significantly impact the quality of life for patients with IBD and impose a socio-economic burden on the healthcare system[4]. Although the precise pathogenesis of IBD remains unclear, the prevailing perspective suggests that it is influenced by genetic susceptibility, immune system dysregulation, alterations in intestinal mucosal permeability, environmental factors, and dietary habits[5,6]. Currently, mesalazine, aminosalicylates, glucocorticoids, and immunosuppressants are widely utilized in the treatment of IBD[7,8].

[1]School of Ocean and Tropical Medicine, Guangdong Medical University, Zhanjiang 524023, China. [2]The Marine Biomedical Research Institute of Guangdong Zhanjiang, Zhanjiang 524023, China. [3]Zhanjiang Engineering Research Center for Algae High-value Utilization, Zhanjiang 524023, China. [4]Guangdong Engineering Technology Research Center for the Development and Utilization of Mangrove Wetland Medicinal Resources, Guangdong Medical University, Zhanjiang 524023, China. [5]Luming Deng, Zhenhui Feng and Xingyan Li contributed equally to this work. ✉email: yehua@gdmu.edu.cn; winokhere@sina.com

Osteoporosis is characterized by low bone mass and the microarchitectural deterioration of bone tissue[9,10]. Emerging evidence has demonstrated that IBD is frequently associated with osteoporosis[11,12]. In patients with IBD, the prevalence of osteoporosis can reach as high as 50%. Moreover, the relative risk of fractures in individuals with IBD increases to approximately 1.3 to 1.4 times that of the general population[13,14]. Clinically, osteoporosis induced by IBD is primarily managed with anti-resorptive agents, such as bisphosphonates, selective estrogen receptor modulators, and anti-RANKL monoclonal antibodies, as well as anabolic agents like human parathyroid hormone analogs and anti-sclerostin monoclonal antibodies[15,16]. However, the efficacy of these medications for IBD and osteoporosis is often limited, and they frequently come with serious side effects[17,18]. Consequently, it is essential to identify safer and more effective natural bioactive compounds for the prevention and treatment of colitis and colitis-associated bone loss.

Phycobiliproteins (PBPs) are a class of natural, nontoxic, water-soluble pigment proteins found in red algae, cyanobacteria, and cryptophytes[19]. Based on their spectral properties, PBPs are typically categorized into four classes: phycoerythrin (PE), phycocyanin (PC), allophycocyanin (APC), and phycoerythrocyanin (PEC)[20]. Notably, PE and PC have garnered significant attention in recent years due to their extensive applications in the food, pharmaceutical, and cosmetic industries[21]. PC is a naturally occurring chromoprotein primarily extracted from Spirulina platensis, comprising α and β subunits[22]. It has been reported that PC exhibits a wide range of bioactivities, including anti-inflammatory, anti-osteoporotic, antioxidant, and anti-tumour properties[23,24]. For instance, Guo et al. demonstrated that PC alleviated colitis in mice via phycocyanobilin-dependent antioxidant and anti-inflammatory mechanisms that protected the intestinal epithelial barrier[25]. Furthermore, AlQranei et al. reported that C-phycocyanin (C-PC) reduced RANKL-induced osteoclastogenesis and bone resorption in vitro by inhibiting ROS levels, NFATc1, and NF-κB activation[26]. PE, another pigment protein, consists of α, β, and γ subunits and can be categorized into three types: R-phycoerythrin (R-PE), C-phycoerythrin (C-PE), and B-phycoerythrin (B-PE), based on their absorption spectra[27]. Among them, B-PE, the major phycobiliprotein of the Porphyridium species, exhibits two absorption peaks at approximately 545 and 565 nm, along with a shoulder peak at around 498 nm, and a fluorescence emission maximum at 580 nm[19]. Our previous study has demonstrated that high-purity B-PE can be recovered from a low concentration of phycobilin in wastewater using a chitosan-based flocculation method, but the bioactivity of B-PE has not yet been evaluated[28].

While previous studies have reported that PC can reduce inflammation and improve bone mass, the effects of B-PE on IBD or osteoporosis have yet to be investigated. Data obtained through network pharmacology and molecular docking indicated that B-PE might ameliorate DSS-induced colitis and colitis-associated bone loss by modulating the PI3K/AKT signaling pathway. Therefore, the objective of this study was to explore the potential therapeutic effects of B-PE on DSS-induced colitis and colitis-associated bone loss, as well as its interaction with the PI3K/AKT signaling pathway. The results showed that B-PE had the potential to attenuate DSS-induced colitis and colitis-associated bone loss by mitigating the inflammatory response, enhancing intestinal barrier function, and stimulating bone formation through the activation of the PI3K/AKT signaling pathway. Collectively, this study provides a theoretical basis for the use of B-PE as a natural bioactive compound to ameliorate colitis and colitis-associated bone loss.

Materials and methods

Materials and reagents

High-purity B-PE was prepared using the method described in our previous study[28]. Dextran Sulfate Sodium Salt (DSS, molecular weight: 36–50 kDa) was purchased from Yeasen Biotechnology Co., Ltd. (Shanghai, China). Calcein and tricaine were procured from Sigma-Aldrich (St. Louis, USA). Hematoxylin and eosin were provided by Beijing Solarbio Science & Technology Co., Ltd. (Beijing, China). The BCA assay kit, RIPA Lysis Buffer, and fat-free powdered milk were obtained from Beyotime Biotech Co., Ltd (Shanghai, China). Primary (GAPDH, ZO-1, E-cadherin, COL1A1, RUNX2, PI3K, p-PI3K, AKT, and p-AKT) and secondary antibodies were purchased from Abcam, Inc. (Shanghai, China). Adult wild-type AB-strain zebrafish were obtained from the Type AB Zebrafish Platform Center of the Guangdong Medical University Affiliated Hospital (Zhanjiang, China). The transgenic zebrafish (Tg, lyz: DsRed) were acquired from the Guangdong Laboratory Animal Monitoring Institute. All other chemicals and reagents were of analytical grade.

Animals and experimental grouping

In this study, zebrafish and their eggs were obtained from the Type AB Zebrafish Platform Center at the Affiliated Hospital of Guangdong Medical University. The zebrafish embryos and larvae were cultured according to our previously described method[29]. Embryos at early larval stages were utilized prior to the determination of sex, resulting in the inclusion of both male and female embryos in the study. After 3 days post-fertilization (dpf), the synchronized embryos were maintained in 24-well plates. Subsequently, the zebrafish larvae were randomly divided into four groups: a control group, a model group (DSS), and two experimental groups (DSS + B-PE 25 μg/mL and DSS + B-PE 100 μg/mL). The control group consisted of zebrafish larvae treated with egg water, while the model group was exposed to 0.5% DSS to induce colitis. Animals in the experimental groups received treatment with 0.5% DSS along with varying concentrations of B-PE (25 and 100 μg/mL). Zebrafish larvae at 9 dpf were collected and then anesthetized with tricaine. Thereafter, changes in zebrafish gut morphology and length were assessed using a spinning disk confocal microscope (SDCM) (Spin SR10, Olympus, Japan). Additionally, the distribution of neutrophils in the intestines of transgenic zebrafish (Tg, lyz: DsRed) was observed using SDCM, and ImageJ was employed for quantitative image analysis. All animal procedures were conducted in accordance with the National Research Council's Guide for the Care and Use of Laboratory Animals Science, which complied with the ARRIVE guidelines and U.S. National Institutes of Health (NIH) Guide for the Care and Use of Laboratory Animals. All experiments were approved by the Institutional Animal Care and Use

Committee (IACUC) of the Guangdong Laboratory Animals Monitoring Institute (Guangzhou, China, NO. A-IACUC2023104).

Hematoxylin and eosin (H&E) staining

Zebrafish larvae were anesthetized using 0.02% tricain and then executed under cryogenic conditions with liquid nitrogen. Subsequently, the larvae, embedded in optimal cutting temperature (OCT) medium, were cut into 8 μm slices using a Leica CM1950 microtome and adhered to glass slides. Standard hematoxylin and eosin (H&E) staining of the paraffin-embedded samples was performed as previously described[30]. Images were captured using a spinning disk confocal microscope (SDCM) (Spin SR10, Olympus, Japan).

Calcein staining

Zebrafish larvae at 9 dpf were collected and then immersed in a 0.2% calcein solution for 15 min. Subsequently, the larvae were thoroughly rinsed with egg water three times, with each wash lasting 10 min. The larvae were then anesthetized using a 0.02% tricaine solution, executed under cryogenic conditions with liquid nitrogen, and subsequently mounted on a depression slide. The zebrafish skulls were scanned using a spinning disk confocal microscope (SDCM) (Spin SR10, Olympus, Japan), while ImageJ was employed for the quantitative analysis of fluorescence images.

qRT-PCR analysis

Zebrafish were anesthetized using 0.02% tricaine and subsequently euthanized under cryogenic conditions with liquid nitrogen. Total RNA was extracted from zebrafish colon tissues using the reagent of Trizol, chloroform, isopropanol, and 75% ethanol. The cDNA synthesis kit (Vazyme Biotech, Nanjing, China) was used to configure the reverse transcription system in accordance with a previous study[31]. All primer sequences were obtained from Sangon Biotech Co., Ltd (Shanghai, China) and were listed in Table 1. Moreover, the relative changes in target gene expression were calculated using the $2^{-\triangle\triangle Ct}$ method and normalized to GAPDH.

Western blot assay

Zebrafish were anesthetized with 0.02% tricaine and subsequently euthanized under cryogenic conditions using liquid nitrogen. Proteins were extracted from zebrafish colon tissues utilizing a lysis buffer at 12,000 rpm for 30 min at 4 °C and quantified employing a BCA protein assay kit. Equal amounts of protein were mixed with SDS–PAGE loading buffer. After quantifying to 40 µg, the samples were separated by 10% SDS–PAGE, and transferred onto PVDF membranes. Following a 2 h blocking period with 5% fat-free milk, the membranes were incubated overnight at 4 °C with primary antibodies (GAPDH, ZO-1, E-cadherin, COL1A1, RUNX2, PI3K, p-PI3K, AKT, and p-AKT). The membranes were then incubated with secondary antibodies for 2 h at room temperature in TBST. Lastly, the protein bands were visualized using the ECL detection system (Beyotime Biotech Co., Ltd, Shanghai, China), and the density of each protein band was quantified using ImageJ software.

Immunofluorescence assay

Colon tissue sections were fixed in acetone for 10 min and subsequently washed three times with PBS. Following this, the sections were blocked with 5% bovine serum albumin (BSA) for 1 h at room temperature and then incubated with primary antibodies (ZO-1 and E-cadherin) overnight at 4 °C. After a 2 h incubation with secondary antibodies at room temperature, the sections were stained with DAPI at room temperature and protected from light for 15 min. The stained sections were observed using SDCM (Spin SR10, Olympus, Japan), and the images were analyzed using ImageJ software.

Network pharmacology analysis

The B-PE targets were obtained from the Swiss Target Prediction database (http://www.swisstargetprediction.ch/) and the PharmMapper database (http://www.lilab-ecust.cn/pharmmapper/). Moreover, the targets associated with IBD and OP were sourced from the GeneCards (https://www.genecards.org/), OMIM (https://omim.org/), and CTD (http://ctdbase.org/) databases using "Osteoporosis" and "Inflammatory bowel disease" as search keywords. Subsequently, all targets related to B-PE, IBD, and OP were imported into a web tool (http://bio

Gene name	NCBI gene accession no.	Primers sequence	
GAPDH	NM_001115114.1	Forward	GTTGTGGAGTCTACTGGTGTCTT
		Reverse	CAGTGCTCATAAGACCTTCAACG
MMP9	NM_213123.1	Forward	GCTCAACCACCGCAGACTAT
		Reverse	GTGCTTCATTGCTGTTCCCG
CXCL8a	XM_009306855.3	Forward	TGTTTTCCTGGCATTTCTGACC
		Reverse	TTTACAGTGTGGGCTTGGAGGG
IL-1β	XM_051908150.1	Forward	GGCTGTGTGTTTGGGAATCT
		Reverse	TGATAAACCAACCGGGACA
TNF-α	NM_212859.2	Forward	CAGGGCAATCAACAAGATGG
		Reverse	TGGTCCTGGTCATCTCTCCA

Table 1. Primer sequences used for qRT-PCR analysis.

informatics.psb.ugent.be/webtools/Venn/) to construct a Venn diagram and identify common targets, which were considered potential targets of B-PE in the treatment of IBD and OP. These targets were then input into the STRING database, with the species set to "*Homo sapiens*". The Protein-Protein Interaction (PPI) network of common targets was visualized using Cytoscape 3.9.1 software. Finally, Gene Ontology (GO) and Kyoto Encyclopedia of Genes and Genomes (KEGG) pathway enrichment analyses[32–34] were conducted using the DAVID platform (https://davidbioinformatics.nih.gov/). The significantly enriched items were subsequently imported into a bioinformatics online platform (http://www.bioinformatics.com.cn/) for visual analysis, and the data were presented as a bubble chart and a histogram.

Molecular docking

Molecular docking can simulate the binding process between components and target proteins, predicting their binding patterns and affinities[35]. In this study, molecular docking was conducted between B-PE and two key proteins in the PI3K/Akt signaling pathway: PI3K and AKT1. The 3D structure of B-PE (3V57) was retrieved from the UniProt database (https://www.uniprot.org), while the X-ray crystal structures of PI3K (7R9V) and AKT1 (5KCV) were obtained from the RCSB Protein Data Bank (PDB). Subsequently, water molecules and small molecule ligands within the structures were removed prior to the addition of hydrogen atoms. The molecular docking of B-PE with PI3K and AKT1 was performed using Discovery Studio2019, and the docking energies were calculated. Finally, the results of the molecular docking were visualized using PyMOL version 2.5.

Statistical analysis

All statistical values were calculated using GraphPad Prism 8.0, and the data were presented as mean value ± standard deviation (SD). The data were analyzed using Student's *t*-tests or one-way analysis of variance (ANOVA). $P < 0.05$ was considered statistically significant.

Results

B-PE attenuates DSS-induced colitis symptoms in zebrafish

Colon length is a widely recognized indicator of the severity of acute colitis in zebrafish. As shown in Fig. 1A and B, the colonic length was significantly reduced following DSS treatment when compared to the control group. However, B-PE treatment significantly inhibited this decrease in colon length. Moreover, H&E staining results

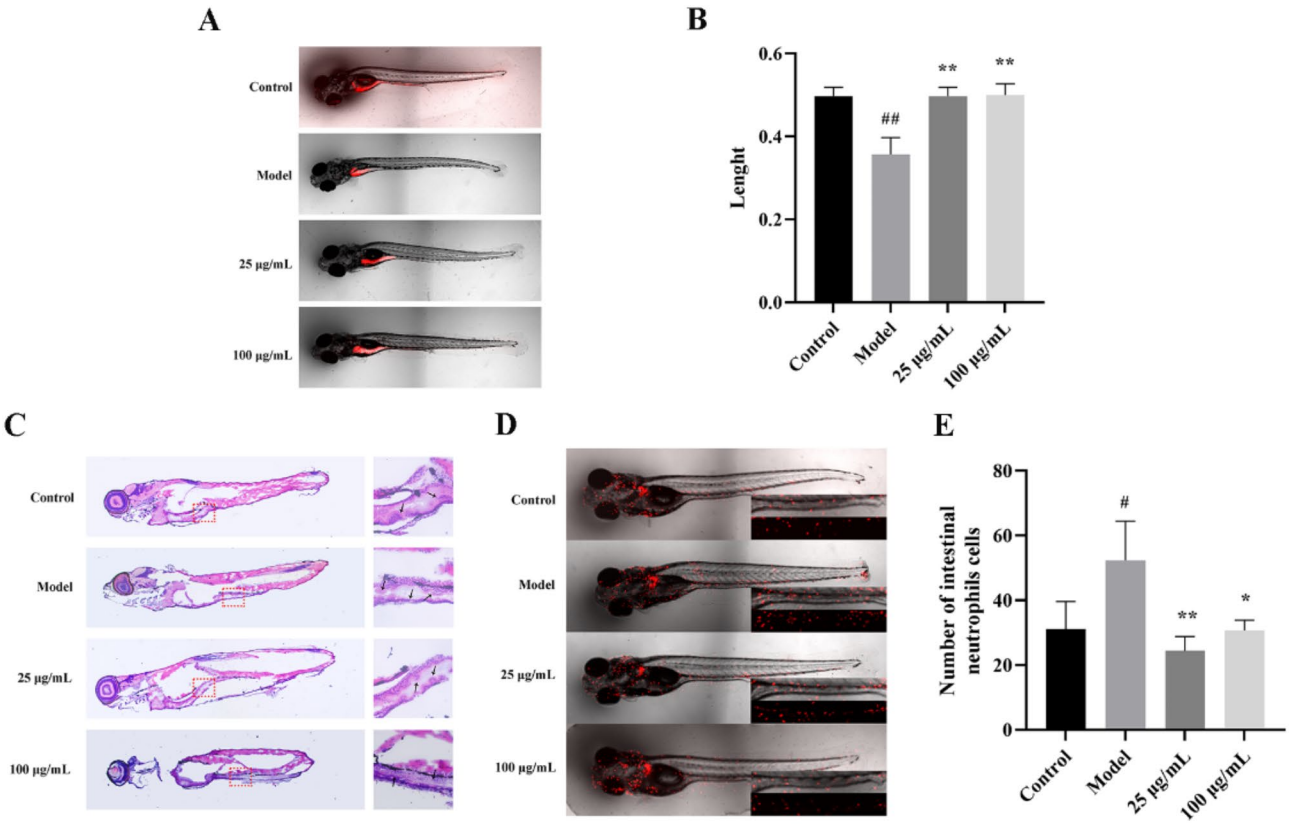

Fig. 1. (**A**) Representative images of the zebrafish colon for each group. (**B**) The colon length of zebrafish across the different groups. (**C**) Representative H&E staining of zebrafish from each group. (**D**) Representative images of intestinal neutrophil cells in zebrafish from each group. (**E**) The quantification of intestinal neutrophil cells in zebrafish for each group. Data are presented as mean ± SD. $^{\#}P < 0.05$ and $^{\#\#}P < 0.01$ *versus* the control group. $^{*}P < 0.05$ and $^{**}P < 0.01$ *versus* the model group.

demonstrated that DSS treatment disrupted the crypt structure and exacerbated inflammatory cell infiltration relative to the control group, whereas B-PE treatment significantly attenuated DSS-induced crypt distortion and inflammation (Fig. 1C). Additionally, as presented in Fig. 1D and E, the number of intestinal neutrophil cells showed a significant increase after DSS treatment compared to the control group, while B-PE treatment significantly reduced the aggregation of intestinal neutrophil cells. These results indicated that B-PE alleviated the symptoms of DSS-induced colitis in zebrafish.

B-PE improves colitis-associated bone loss in zebrafish

Calcein is a fluorescent dye that binds to the calcified bone matrix and is frequently employed for staining the entire skeleton of zebrafish[36]. As illustrated in Fig. 2A and D, the number of mineralized tissue stains in the zebrafish skull was significantly reduced by DSS compared to the control group. In contrast, B-PE treatment resulted in a significant increase in the number of mineralized tissue stains. Furthermore, the relative fluorescence intensity and area of the zebrafish skulls were quantified, as shown in Fig. 2E and F. The groups treated with B-PE displayed a significant dose-dependent increase in both the relative fluorescence intensity and the area of the zebrafish skulls. These findings indicated that B-PE effectively promoted osteogenic mineralization, thereby ameliorating colitis-associated bone loss. Collectively, the above results suggested that B-PE had the potential to improve colitis and colitis-associated bone loss in DSS-induced colitis zebrafish.

Network pharmacology analysis and molecular docking

To explore the potential mechanisms by which B-PE may treat colitis and colitis-associated bone loss, we conducted a network pharmacology analysis. After eliminating duplicates, we identified a total of 286 targets associated with B-PE from the Swiss Target Prediction and PharmMapper databases. Additionally, we collected 3908 targets related to OP and 3499 targets associated with IBD from the GeneCards, OMIM, and CTD databases after eliminating duplicates, respectively. Consequently, Venny analysis, as illustrated in Fig. 3A, revealed 99 common targets. These common targets were subsequently imported into the STRING database to construct the PPI network. Visualization of the PPI network was performed using Cytoscape 3.9.1 software, which highlighted the top 10 most significant targets based on degree value: TNF, AKT1, EGFR, CASP3, ESR1, MMP9, MAPK3, SRC, MMP2, and MTOR, as shown in Fig. 3B.

To evaluate the potential influence of B-PE on common target-related signaling pathways, the Metascape database was used for GO and KEGG enrichment analyses of 99 common targets. As shown in Fig. 3C, the biological progress (BP) primarily encompassed protein phosphorylation, positive regulation of protein kinase B signaling, insulin receptor signaling pathway, extracellular matrix disassembly, and cellular response to reactive oxygen species. The cellular components (CC) predominantly included the cytoplasm, plasma membrane, extracellular region, cell surface, and macromolecular complex. Moreover, the enrichment terms for molecular functions (MF) were chiefly associated with protein tyrosine kinase activity, enzyme binding, ATP binding, protein kinase activity, and protein binding. Results from the KEGG enrichment analysis suggested that the signaling pathways implicated in the treatment of colitis and colitis-associated bone loss by B-PE primarily included the PI3K/Akt signaling pathway, Chemokine signaling pathway, MAPK signaling pathway, Relaxin signaling pathway, and Endocrine resistance (Fig. 3D). Given the significant enrichment of the PI3K/AKT signaling pathway and the identification of AKT1 as a common target, we propose that B-PE could potentially ameliorate DSS-induced colitis and colitis-associated bone loss through modulation of the PI3K/AKT signaling pathway.

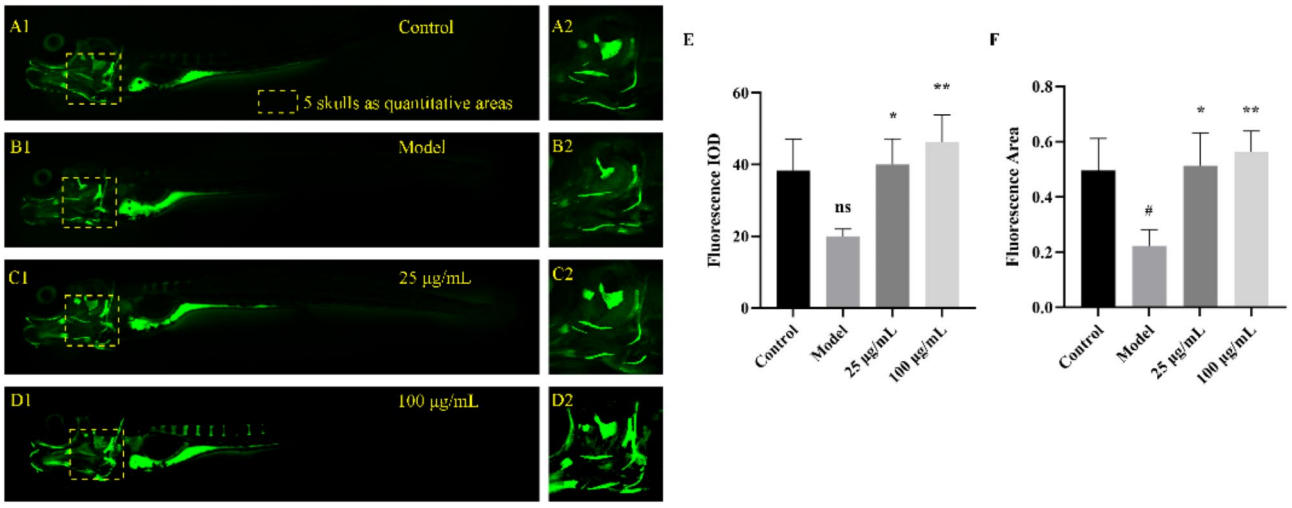

Fig. 2. ($\mathbf{A_1}$–$\mathbf{D_1}$) Fluorescence images depicting the entire zebrafish skeleton at 4× magnification. ($\mathbf{A_2}$–$\mathbf{D_2}$) Fluorescence intensity images of zebrafish skulls at 20× magnification. (**E**) Quantification of the relative fluorescence intensity of zebrafish skulls. (**F**) Quantification of the fluorescence area of zebrafish skulls. Data are presented as mean ± SD. $^{\#}P < 0.05$ *versus* the control group. $^{*}P < 0.05$ and $^{**}P < 0.01$ *versus* the model group.

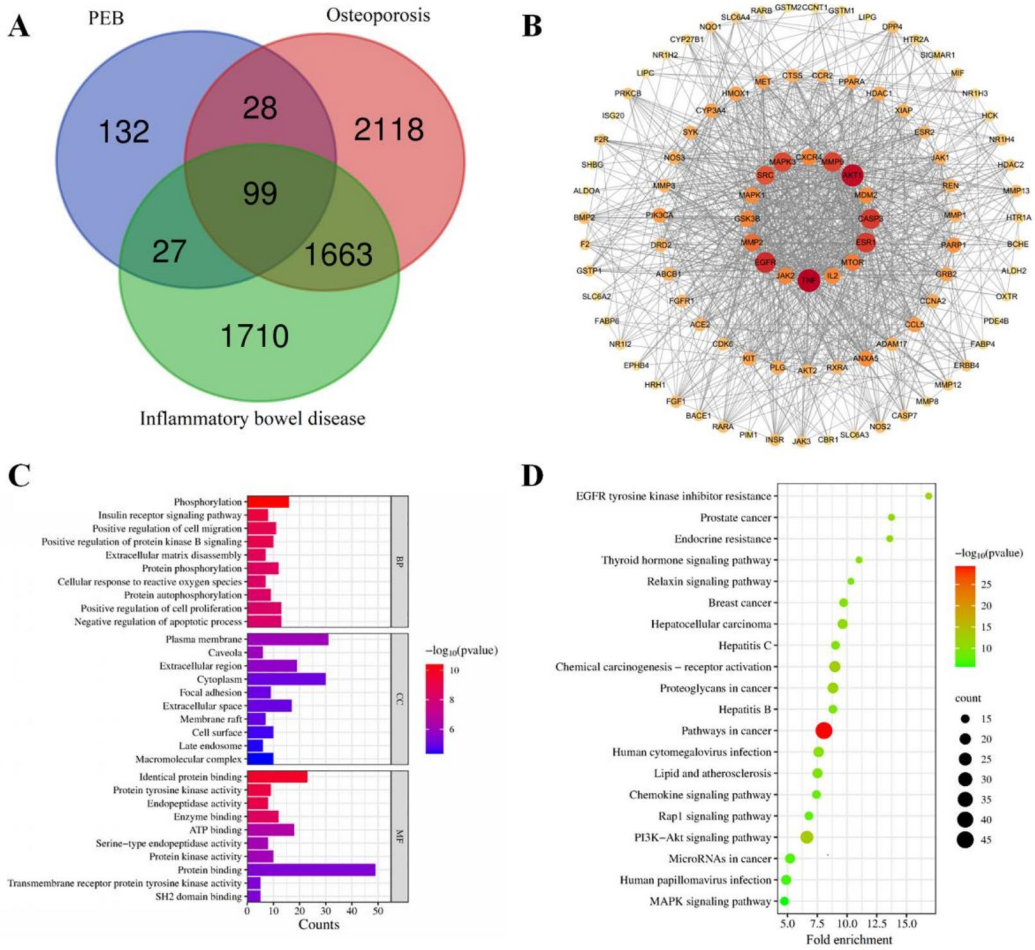

Fig. 3. Network pharmacology analysis of B-PE against OP and IBD. (**A**) Common targets of B-PE, OP, and IBD. (**B**) PPI network of common targets. (**C**) GO enrichment analysis of common targets. (**D**) KEGG enrichment analysis of common targets.

Subsequently, molecular docking was conducted to investigate the potential interactions between B-PE and PI3K, as well as AKT1 (Fig. 4). The binding energy was calculated to assess the affinity between the compound and target proteins, with lower binding energy indicating a stronger affinity. The results of the molecular docking revealed binding energies of -20.72 kcal/mol for B-PE with PI3K and – 15.46 kcal/mol with AKT1, demonstrating a good affinity between B-PE and both proteins. Collectively, these findings suggested that B-PE may exert its therapeutic effects on colitis and colitis-associated bone loss via the PI3K/AKT signaling pathway.

B-PE reduces inflammatory response in DSS-induced colitis zebrafish

Pro-inflammatory cytokines, such as interleukin-1β (IL-1β) and tumor necrosis factor α (TNF-α), play a crucial role in DSS-induced colitis, with the majority being produced by macrophages[37]. To investigate the effects of B-PE on pro-inflammatory cytokines in DSS-induced colitis, the mRNA levels of TNF-α and IL-1β in colon tissues were evaluated using qRT-PCR. In this study, significantly elevated levels of TNF-α and IL-1β were observed in the DSS-treated model group compared to the control group, whereas B-PE treatment significantly decreased the mRNA levels of TNF-α (Fig. 5A) and IL-1β (Fig. 5B) in a dose-dependent manner. Matrix metalloproteinase-9 (MMP9), a member of the MMP family, has been reported to be closely associated with inflammation-related diseases[38,39]. As shown in Fig. 5C, following DSS induction, the mRNA level of MMP9 was significantly higher compared to the control group. However, B-PE treatment significantly down-regulated the mRNA level of MMP9 in a dose-dependent manner. CXCL8a, also known as interleukin-8 (IL-8), is an important inflammatory CXC chemokine that plays a key role in inflammation and the immune response by attracting neutrophils to sites of inflammation[40,41]. As depicted in Fig. 5D, DSS significantly increased the mRNA level of CXCL8a compared to the control group, while B-PE treatment significantly reversed the up-regulation of CXCL8a induced by DSS. Collectively, these results demonstrated that B-PE had the potential to be a potent anti-inflammatory agent, ameliorating the inflammatory response in DSS-induced colitis.

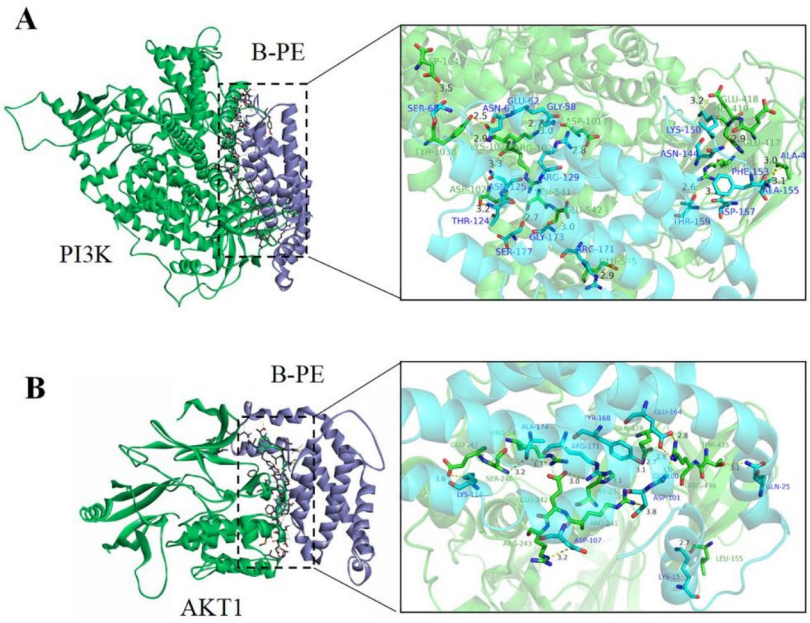

Fig. 4. Molecular docking of B-PE with PI3K (**A**) and AKT1 (**B**).

B-PE enhances the intestinal barrier function in DSS-induced colitis zebrafish

Tight junction proteins and adherens junction proteins, including zonula occluden-1 (ZO-1) and E-cadherin, are essential for maintaining the intestinal epithelial barrier function[42,43]. To further evaluate the effects of B-PE on the intestinal barrier in DSS-induced colitis, the expressions of ZO-1 and E-cadherin were quantified using a western blot assay. As illustrated in Fig. 6A and B, DSS significantly down-regulated the expression of ZO-1 and E-cadherin in colon tissues compared to the control group. Conversely, the B-PE treatment groups exhibited a dose-dependent increase in the expressions of ZO-1 and E-cadherin relative to the model group. Additionally, the results from the immunofluorescence assay showed that B-PE treatment significantly up-regulated the expressions of ZO-1 and E-cadherin in a dose-dependent manner when compared to the model group (Fig. 6C and D). These findings suggested that B-PE improved DSS-induced impairment of intestinal epithelial barrier function in zebrafish.

B-PE up-regulates the expression levels of osteogenesis-related proteins

To evaluate the effects of B-PE on colitis-associated bone loss in zebrafish, the expression of osteogenesis-related proteins (COL1A1 and RUNX2) was assessed using a western blot assay. As shown in Fig. 7, the expression levels of COL1A1 and RUNX2 were reduced in the DSS model groups compared to the control group. However, B-PE treatment significantly up-regulated the expression levels of COL1A1 and RUNX2 in a dose-dependent manner relative to the model group. Thus, these data indicated that B-PE improved colitis-associated bone loss by stimulating bone formation.

B-PE ameliorates DSS-induced colitis and colitis-associated bone loss by activating the PI3K/AKT signaling pathway

Based on the results of network pharmacology analysis and KEGG pathway enrichment, we further investigated the potential mechanism by which B-PE ameliorated DSS-induced colitis and colitis-associated bone loss via the PI3K/AKT signaling pathway, utilizing a western blot assay. As shown in Fig. 8, the levels of phosphorylated PI3K and AKT (p-PI3K/PI3K and p-AKT/AKT) in the model group were significantly lower compared to the control group. In contrast, treatment with B-PE markedly increased the expression levels of phosphorylated PI3K and AKT (p-PI3K/PI3K and p-AKT/AKT) when compared to the model group. These results indicated

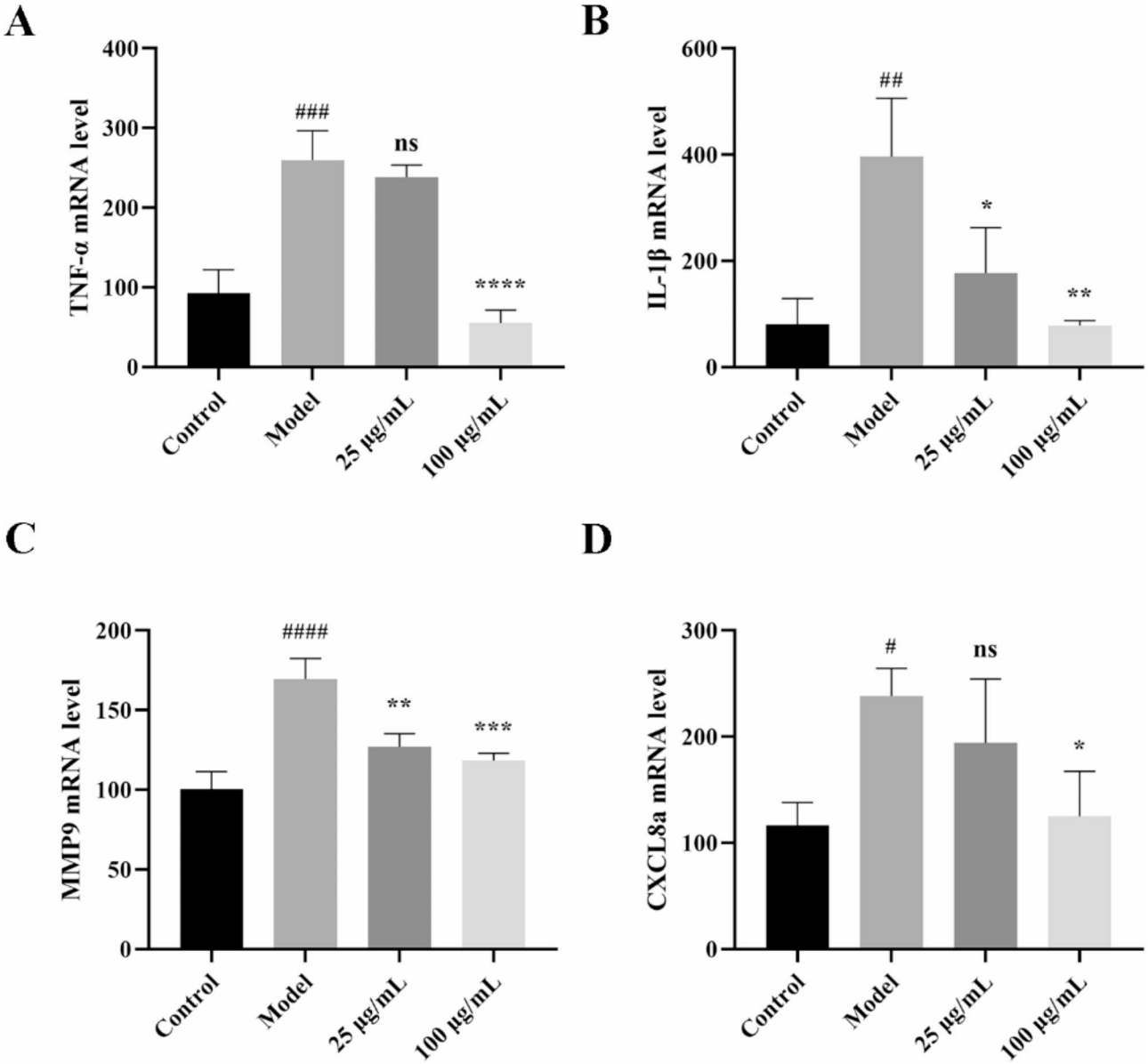

Fig. 5. The relative mRNA levels of TNF-α (**A**), IL-1β (**B**), MMP9 (**C**), and CXCL8a (**D**) were quantified using qRT-PCR. Data are presented as mean ± SD. $^{\#}P < 0.05$, $^{\#\#}P < 0.01$, $^{\#\#\#}P < 0.001$, and $^{\#\#\#\#}P < 0.0001$ *versus* the control group. $^{*}P < 0.05$, $^{**}P < 0.01$, $^{***}P < 0.001$, and $^{****}P < 0.0001$ *versus* the model group.

that B-PE could alleviate DSS-induced colitis and colitis-associated bone loss by activating the PI3K-AKT signaling pathway.

Discussion

IBD is a disorder that affects the gastrointestinal tract and encompasses both CD and UC[44]. Research indicates a significant correlation between IBD and OP, with up to 50% of IBD patients affected by OP[12,14]. Furthermore, the relative risk of fracture in these patients is elevated by approximately 1.3 to 1.4 times, which poses substantial economic and healthcare challenges for society[14]. Currently, limited therapeutic options are available for both IBD and OP, and some medications carry potential serious side effects associated with long-term use. Therefore, there is a critical need to explore new therapeutic approaches for IBD and OP. Recent studies have demonstrated that PC, a pigment protein, exhibits anti-colitis effects through its antioxidant and anti-inflammatory mechanisms[25]. Additionally, PC has been shown to inhibit RANKL-induced osteoclastogenesis by suppressing the activation of NFATc1 and c-Fos[26]. However, the effects of B-PE, another pigment protein, on colitis and colitis-associated bone loss, as well as its underlying mechanisms, remain unclear. In this study, the colitis zebrafish model was induced using DSS. Subsequently, we found that DSS exacerbated inflammatory cell infiltration and increased intestinal neutrophil aggregation, whereas B-PE significantly reversed these alterations. Moreover, DSS treatment resulted

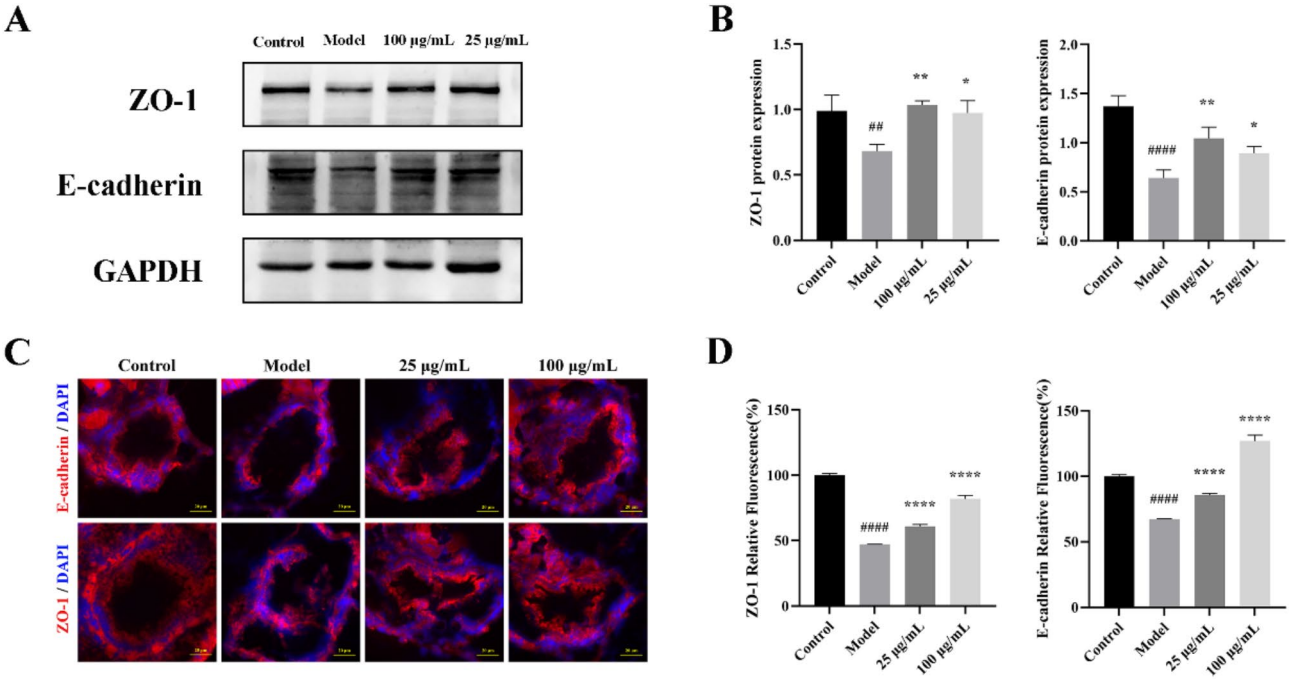

Fig. 6. (**A**) Western blot analysis of ZO-1 and E-cadherin proteins expressions. (**B**) Quantification of ZO-1 and E-cadherin proteins expressions levels. (**C**) Images of immunofluorescence staining in zebrafish colon tissues. (**D**) Quantification of the relative fluorescence intensity of ZO-1 and E-cadherin. Data are presented as mean ± SD. $^{\#\#}P < 0.01$ and $^{\#\#\#\#}P < 0.0001$ *versus* the control group. $^{*}P < 0.05$, $^{**}P < 0.01$, and $^{****}P < 0.0001$ *versus* the model group.

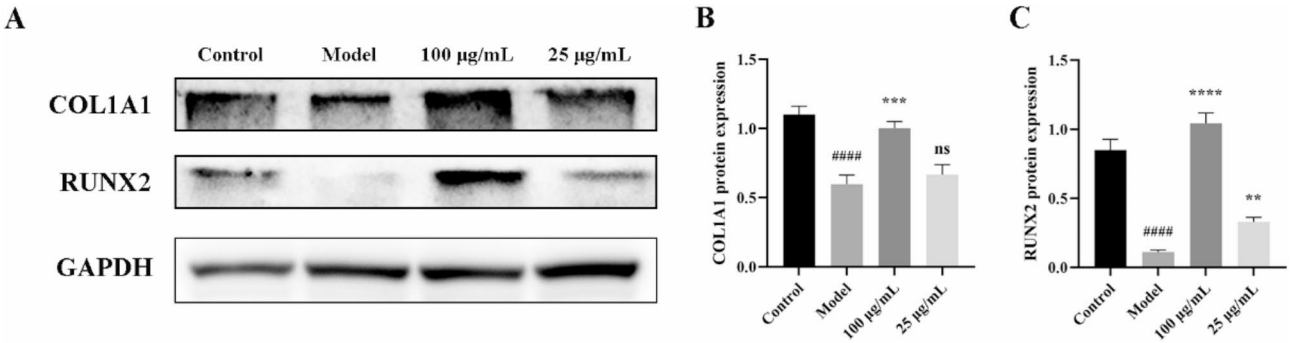

Fig. 7. (**A**) Western blot analysis of COL1A1 and RUNX2 proteins expressions. (**B**) Quantification of COL1A1 protein expression level. (**C**) Quantification of RUNX2 protein expression level. Data are presented as mean ± SD. $^{\#\#\#\#}P < 0.0001$ *versus* the control group. $^{**}P < 0.01$, $^{***}P < 0.001$, and $^{****}P < 0.0001$ *versus* the model group.

in bone loss in zebrafish, while B-PE administration promoted osteogenic mineralization. The above results implied that B-PE could ameliorate DSS-induced colitis and colitis-associated bone loss.

Network pharmacology analysis is an emerging interdisciplinary approach that examines the interactions among drugs, targets, and diseases, thereby providing insights into the underlying molecular mechanisms by which drugs treat diseases[45]. Molecular docking is a powerful tool for investigating molecular interactions and has been extensively utilized in drug discovery. A lower binding energy indicates that less energy is required for the docking structure, suggesting a higher likelihood and stability of the compound binding to the target[46,47]. To explore the potential mechanism of B-PE on colitis and colitis-associated bone loss, network pharmacology analysis and molecular docking were performed, resulting in the identification of 99 common targets of B-PE against IBD and OP. PPI network analysis suggested that B-PE may improve colitis and colitis-associated bone loss by regulating TNF, AKT1, EGFR, CASP3, ESR1, MMP9, MAPK3, SRC, MMP2, and MTOR. GO enrichment analysis indicated that the biological processes enriched in the common targets primarily included protein phosphorylation and positive regulation of protein kinase B signaling. Furthermore, the molecular function enrichment terms were predominantly associated with protein tyrosine kinase activity, protein kinase activity,

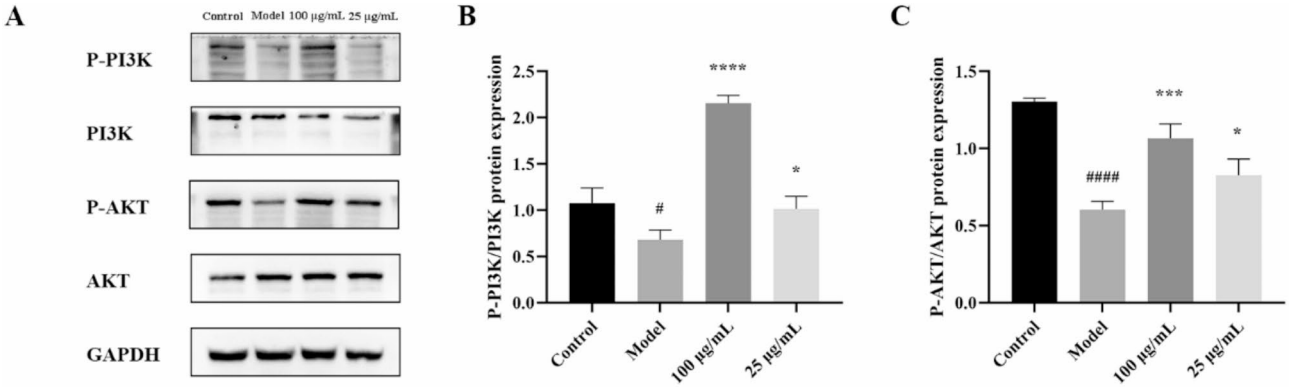

Fig. 8. (**A**) Western blot analysis of p-PI3K, PI3K, p-AKT, and AKT proteins expressions. (**B**) Quantification of p-PI3K protein expression level normalized by PI3K. (**C**) Quantification of p-AKT protein expression level normalized by AKT. Data are presented as mean ± SD. $^{\#}P < 0.05$ and $^{\#\#\#\#}P < 0.0001$ *versus* the control group. $^{*}P < 0.05$, $^{***}P < 0.001$, and $^{****}P < 0.0001$ *versus* the model group.

and protein binding. Additionally, KEGG pathway enrichment analysis demonstrated that B-PE may play a crucial role in modulating the PI3K/AKT signaling pathway. Subsequent molecular docking results revealed that B-PE exhibited good affinity for both PI3K and AKT1, with binding energies of -20.72 kcal/mol and – 15.46 kcal/mol, respectively. Collectively, these results demonstrated that the PI3K/AKT signaling pathway may represent a potential signaling pathway for B-PE in the treatment of colitis and colitis-associated bone loss.

The PI3K/AKT signaling pathway regulates various cellular biological processes, including cell proliferation, survival, apoptosis, and metabolism, through the activation of PI3K and subsequent phosphorylation of AKT[48,49]. Studies have shown that the PI3K/AKT signaling pathway plays a crucial role in the development of OP and IBD[50,51]. Chen et al. discovered that andrographolide, a diterpenoid lactone extracted from *Andrographis paniculata Nees*, promoted bone formation and inhibited bone loss in glucocorticoid-induced osteoporosis by activating the PI3K/AKT signaling pathway[52]. Moreover, luteolin, a flavonoid, has been reported to stimulate the osteogenic differentiation of bone marrow mesenchymal stem cells (BMSCs) through the activation of PI3K/AKT signaling pathway, thereby exerting an anti-OP effect[53]. In this study, we observed that the levels of p-PI3K and p-AKT decreased following DSS treatment, whereas B-PE significantly activated the PI3K/AKT signaling pathway. Furthermore, B-PE markedly increased the expression of osteogenic markers COL1A1 and RUNX2. Previous research has indicated that the overexpression of RUNX2 enhanced the osteogenic potential of BMSCs[54]. Consequently, RUNX2 is recognized as a major regulator of bone formation and osteogenic differentiation. During the process of osteoblast differentiation, RUNX2 modulates the expression of various osteogenesis-related proteins, including RUNX2, COL1A1, and OCN, thereby promoting osteogenic differentiation[55]. Collectively, our results indicated that B-PE treatment significantly enhanced osteogenesis through the activation of the PI3K/AKT signaling pathway. Additionally, prior studies have demonstrated that the activation of the PI3K/AKT signaling pathway can inhibit NF-κB activation, resulting in decreased expression of pro-inflammatory cytokines such as IL-1β and TNF-α, ultimately leading to a reduction in the inflammatory response[49,51]. Consistent with these findings, our results revealed that B-PE dose-dependently reduced the mRNA levels of TNF-α, IL-1β, MMP9, and CXCL8a via the activation of the PI3K/AKT signaling pathway. Moreover, ZO-1 and E-cadherin are essential for maintaining intestinal barrier function. Studies have shown that increasing the expression levels of ZO-1 and E-cadherin can enhance this function[56,57]. In the present study, we found that B-PE significantly increased the expression of ZO-1 and E-cadherin in a dose-dependent manner, leading to improved intestinal barrier function.

Conclusion

In summary, to investigate the potential mechanism of B-PE in treating colitis and colitis-associated bone loss, we conducted a combination of network pharmacology analysis, molecular docking, and experimental validation. The findings suggested that B-PE could attenuate colitis and colitis-associated bone loss by reducing the inflammatory response, protecting intestinal barrier function, and promoting bone formation through the activation of the PI3K/AKT signaling pathway. Taken together, this study provides valuable evidence supporting the use of B-PE as a promising therapeutic candidate for the treatment of colitis and colitis-associated bone loss. Future investigations should prioritize the validation of other relevant targets and signaling pathways predicted by network pharmacology in the treatment of OP and IBD with B-PE.

Data availability

The authors declare that the data supporting the findings of this study are available within the paper and its Supplementary Information files.

Received: 12 August 2024; Accepted: 10 February 2025
Published online: 14 February 2025

References

1. Luo, H. et al. Emerging pharmacotherapy for inflammatory bowel diseases. *Pharmacol. Res.* **178**, 106146. https://doi.org/10.1016/j.phrs.2022.106146 (2022).
2. Neurath, M. F. Cytokines in inflammatory bowel disease. *Nat. Rev. Immunol.* **14**, 329–342. https://doi.org/10.1038/nri3661 (2014).
3. Zhang, S. X., Liang, Y. J., Yao, J., Li, D. F. & Wang, L. S. Role of pyroptosis in inflammatory bowel disease (IBD): from gasdermins to DAMPs. *Front. Pharmacol.* **13**, 833588. https://doi.org/10.3389/fphar.2022.833588 (2022).
4. Katsandegwaza, B., Horsnell, W. & Smith, K. Inflammatory bowel disease: a review of pre-clinical murine models of human disease. *Int. J. Mol. Sci.* **23**, 9344. https://doi.org/10.3390/ijms23169344 (2022).
5. Dong, Y. M., Xu, T. G., Xiao, G. Z., Hu, Z. Y. & Chen, J. Y. Opportunities and challenges for synthetic biology in the therapy of inflammatory bowel disease. *Front. Bioeng. Biotech.* **10**, 909591. https://doi.org/10.3389/fbioe.2022.909591 (2022).
6. Zhang, H. M. et al. Stem cell-based therapies for inflammatory bowel disease. *Int. J. Mol. Sci.* **23**, 8494. https://doi.org/10.3390/ijms23158494 (2022).
7. Zheng, M. Y. et al. The role of *Akkermansia muciniphila* in inflammatory bowel disease: current knowledge and perspectives. *Front. Immunol.* **13**, 1089600. https://doi.org/10.3389/fimmu.2022.1089600 (2023).
8. Yasmin, F. et al. Novel drug delivery systems for inflammatory bowel disease. *World J. Gastroentero.* 28, (1922). https://doi.org/10.3748/wjg.v28.i18.1922 (2022).
9. Rachner, T. D., Khosla, S. & Hofbauer, L. C. Osteoporosis: now and the future. *Lancet* **377**, 1276–1287. https://doi.org/10.1016/S0140-6736(10)62349-5 (2011).
10. Harvey, N., Dennison, E. & Cooper, C. Osteoporosis: impact on health and economics. *Nat. Rev. Rheumatol.* **6**, 99–105. https://doi.org/10.1038/nrrheum.2009.260 (2010).
11. Lima, C. A., Lyra, A. C., Rocha, R. & Santana, G. O. Risk factors for osteoporosis in inflammatory bowel disease patients. *World J. Gastrointest. Pathophysiol.* **6**, 210–218. https://doi.org/10.4291/wjgp.v6.i4.210 (2015).
12. Reinshagen, M. Osteoporosis in inflammatory bowel disease. *J. Crohns Colitis.* **2**, 202–207. https://doi.org/10.1016/j.crohns.2008.01.005 (2008).
13. Targownik, L. E., Bernstein, C. N. & Leslie, W. D. Inflammatory bowel disease and the risk of osteoporosis and fracture. *Maturitas* **76**, 315–319. https://doi.org/10.1016/j.maturitas.2013.09.009 (2013).
14. Tilg, H., Moschen, A. R., Kaser, A., Pines, A. & Dotan, I. Gut, inflammation and osteoporosis: basic and clinical concepts. *Gut* **57**, 684–694. https://doi.org/10.1136/gut.2006.117382 (2008).
15. Song, S. S., Guo, Y. Y., Yang, Y. H. & Fu, D. H. Advances in pathogenesis and therapeutic strategies for osteoporosis. *Pharmacol. Therapeut.* **237**, 108168. https://doi.org/10.1016/j.pharmthera.2022.108168 (2022).
16. Li, S. S. et al. Recent progresses in the treatment of osteoporosis. *Front. Pharmacol.* **12**, 717065. https://doi.org/10.3389/fphar.2021.717065 (2021).
17. Grossberg, L. B., Papamichael, K. & Cheifetz, A. S. Emerging drug therapies in inflammatory bowel disease. *Aliment. Pharm. Ther.* **55**, 789–804. https://doi.org/10.1111/apt.16785 (2022).
18. Vidal, M., Thibodaux, R. J., Neira, L. F. V. & Messina, O. D. Osteoporosis: a clinical and pharmacological update. *Clin. Rheumatol.* **38**, 385–395. https://doi.org/10.1007/s10067-018-4370-1 (2019).
19. Tang, Z. H. et al. One-step chromatographic procedure for purification of B-phycoerythrin from *Porphyridium cruentum*. *Protein Expres Purif.* **123**, 70–74. https://doi.org/10.1016/j.pep.2016.01.018 (2016).
20. Munier, M. et al. Physicochemical factors affecting the stability of two pigments: R-phycoerythrin of *Grateloupia turuturu* and B-phycoerythrin of *Porphyridium cruentum*. *Food Chem.* **150**, 400–407. https://doi.org/10.1016/j.foodchem.2013.10.113 (2014).
21. Patel, S. N. et al. Antioxidant activity and associated structural attributes of *Halomicronema phycoerythrin*. *Int. J. Biol. Macromol.* **111**, 359–369. https://doi.org/10.1016/j.ijbiomac.2017.12.170 (2018).
22. Liu, Q., Li, W. J. & Qin, S. Therapeutic effect of phycocyanin on acute liver oxidative damage caused by X-ray. *Biomed. Pharmacother.* **130**, 110553. https://doi.org/10.1016/j.biopha.2020.110553 (2020).
23. Xiang, X. et al. Study on promoting regeneration of zebrafish skull by phycocyanin characterized by in vivo optical coherence tomography. *J. Biophotonics*. **15**, e202100333. https://doi.org/10.1002/jbio.202100333 (2022).
24. Cherng, S. C., Cheng, S. N., Tarn, A. & Chou, T. C. Anti-inflammatory activity of c-phycocyanin in lipopolysaccharide-stimulated RAW 264.7 macrophages. *Life Sci.* **81**, 1431–1435. https://doi.org/10.1016/j.lfs.2007.09.009 (2007).
25. Guo, W. et al. Phycocyanin ameliorates mouse colitis *via* phycocyanobilin-dependent antioxidant and anti-inflammatory protection of the intestinal epithelial barrier. *Food Funct.* **13**, 3294–3307. https://doi.org/10.1039/D1FO02970C (2022).
26. AlQranei, M. S., Aljohani, H., Majumdar, S., Senbanjo, L. T. & Chellaiah, M. A. C-phycocyanin attenuates RANKL-induced osteoclastogenesis and bone resorption in vitro through inhibiting ROS levels, NFATc1 and NF-κB activation. *Sci. Rep.* **10**, 2513. https://doi.org/10.1038/s41598-020-59363-y (2020).
27. Meng, D. M. et al. Self-assembly of phycoerythrin with oligochitosan by electrostatic interaction for stabilization of phycoerythrin. *J. Agric. Food Chem.* **69**, 12818–12827. https://doi.org/10.1021/acs.jafc.1c05205 (2021).
28. Liang, Y. Y. et al. A chitosan-based flocculation method for efficient recovery of high-purity B-phycoerythrin from a low concentration of phycobilin in wastewater. *Molecules* **28**, 3600. https://doi.org/10.3390/molecules28083600 (2023).
29. Li, X. J. et al. Structural characterization of a mannoglucan polysaccharide from *Dendrobium huoshanense* and evaluation of its osteogenesis promotion activities. *Int. J. Biol. Macromol.* **211**, 441–449. https://doi.org/10.1016/j.ijbiomac.2022.05.036 (2022).
30. Feng, J. H., Zhang, L. N., Tang, X., Hu, W. & Zhou, P. Major yolk protein from sea cucumber (Stichopus japonicus) attenuates acute colitis via regulation of microbial dysbiosis and inflammatory responses. *Food Res. Int.* **151**, 110841. https://doi.org/10.1016/j.foodres.2021.110841 (2022).
31. Zhao, Q. N. et al. Hypoglycemic effect and intestinal transport of phenolics-rich extract from digested mulberry leaves in Caco-2/insulin-resistant HepG2 co-culture model. *Food Res. Int.* **175**, 113689. https://doi.org/10.1016/j.foodres.2023.113689 (2024).
32. Kanehisa, M. & Goto, S. K. E. G. G. Kyoto encyclopedia of genes and genomes. *Nucleic Acids Res.* **28**, 27–30. https://doi.org/10.1093/nar/28.1.27 (2000).
33. Kanehisa, M. Toward understanding the origin and evolution of cellular organisms. *Protein Sci.* **28**, 1947–1951. https://doi.org/10.1002/pro.3715 (2019).
34. Kanehisa, M., Furumichi, M., Sato, Y., Matsuura, Y. & Ishiguro-Watanabe, M. KEGG: biological systems database as a model of the real world. *Nucleic Acids Res.* **53**, D672–D677. https://doi.org/10.1093/nar/gkae909 (2025).
35. Liu, J. H. et al. Network pharmacology, molecular docking, and experimental verification reveal the mechanism of San-Huang decoction in treating acute kidney injury. *Front. Pharmacol.* **14**, 1060464. https://doi.org/10.3389/fphar.2023.1060464 (2023).
36. Zhang, S. J., Zhang, Q., Zhang, D. W., Wang, C. S. & Yan, C. Y. Anti-osteoporosis activity of a novel *Achyranthes bidentata* polysaccharide via stimulating bone formation. *Carbohyd Polym.* **184**, 288–298. https://doi.org/10.1016/j.carbpol.2017.12.070 (2018).
37. Yin, Q. et al. An immuno-blocking agent targeting IL-1β and IL-17A reduces the lesion of DSS-induced ulcerative colitis in mice. *Inflammation* **44**, 1724–1736. https://doi.org/10.1007/s10753-021-01449-4 (2021).
38. Takai, S. & Jin, D. N. Pathophysiological role of chymase-activated matrix metalloproteinase-9. *Biomedicines* **10**, 2499. https://doi.org/10.3390/biomedicines10102499 (2022).
39. Li, T. W. et al. The role of matrix metalloproteinase-9 in atherosclerotic plaque instability. *Mediat. Inflamm.* 3872367. (2020). https://doi.org/10.1155/2020/3872367 (2020).

40. Koubourli, D. V., Yaparla, A., Popovic, M. & Grayfer, L. Amphibian (*Xenopus laevis*) interleukin-8 (CXCL8): a perspective on the evolutionary divergence of granulocyte chemotaxis. *Front. Immunol.* 9, (2058). https://doi.org/10.3389/fimmu.2018.02058 (2018).
41. Powell, D. et al. Chemokine signaling and the regulation of bidirectional leukocyte migration in interstitial tissues. *Cell. Rep.* **19**, 1572–1585. https://doi.org/10.1016/j.celrep.2017.04.078 (2017).
42. Jiang, S. S., Xu, H. N., Zhao, C. H., Zhong, F. & Li, D. Oyster polysaccharides relieve DSS-induced colitis via anti-inflammatory and maintaining the physiological hypoxia. *Int. J. Biol. Macromol.* **238**, 124150. https://doi.org/10.1016/j.ijbiomac.2023.124150 (2023).
43. Cai, Y. J. et al. KGF inhibits hypoxia-induced intestinal epithelial cell apoptosis by upregulating AKT/ERK pathway-dependent E-cadherin expression. *Biomed. Pharmacother.* **105**, 1318–1324. https://doi.org/10.1016/j.biopha.2018.06.091 (2018).
44. Del Sordo, R., Lougaris, V., Bassotti, G., Armuzzi, A. & Villanacci, V. Therapeutic agents affecting the immune system and drug-induced inflammatory bowel disease (IBD): a review on etiological and pathogenetic aspects. *Clin. Immunol.* **234**, 108916. https://doi.org/10.1016/j.clim.2021.108916 (2022).
45. Zhao, L. et al. Network pharmacology, a promising approach to reveal the pharmacology mechanism of Chinese medicine formula. *J. Ethnopharmacol.* **309**, 116306. https://doi.org/10.1016/j.jep.2023.116306 (2023).
46. Jia, M. J., Yang, X., Bao, Y. H. & Huo, J. W. Anti-osteoporosis effect of *Mori Follum-Portulaca oleracea* L.-*Lycium barbarum* L. extract based on network pharmacology and experimental validation and its utilization in functional yogurt. *Food Biosci.* **59**, 103974. https://doi.org/10.1016/j.fbio.2024.103974 (2024).
47. Chen, S. N., Li, B., Chen, L. & Jiang, H. L. Uncovering the mechanism of resveratrol in the treatment of diabetic kidney disease based on network pharmacology, molecular docking, and experimental validation. *J. Transl Med.* **21**, 380. https://doi.org/10.1186/s12967-023-04233-0 (2023).
48. Zuo, H. J. et al. Gastrodin regulates PI3K/AKT-Sirt3 signaling pathway and proinflammatory mediators in activated microglia. *Mol. Neurobiol.* **61**, 2728–2744. https://doi.org/10.1007/s12035-023-03743-8 (2024).
49. Yang, P. et al. Gastrodin attenuation of the inflammatory response in H9c2 cardiomyocytes involves inhibition of NF-κB and MAPKs activation via the phosphatidylinositol 3-kinase signaling. *Biochem. Pharmacol.* **85**, 1124–1133. https://doi.org/10.1016/j.bcp.2013.01.020 (2013).
50. Zhang, H. H. et al. Integration of network pharmacology and experimental validation to explore the pharmacological mechanisms of Zhuanggu Busui formula against osteoporosis. *Front. Endocrinol.* **12**, 841668. https://doi.org/10.3389/fendo.2021.841668 (2022).
51. Zhang, B. B. et al. Arbutin attenuates LPS-induced acute kidney injury by inhibiting inflammation and apoptosis via the PI3K/Akt/Nrf2 pathway. *Phytomedicine* **82**, 153466. https://doi.org/10.1016/j.phymed.2021.153466 (2021).
52. Chen, M. et al. Andrographolide protects BMSCs from dexamethasone-induced cellular dysfunction and promotes bone formation via the PI3K/AKT pathway. *J. Funct. Foods.* **105**, 105576. https://doi.org/10.1016/j.jff.2023.105576 (2023).
53. Liang, G. H. et al. Mechanism and experimental verification of luteolin for the treatment of osteoporosis based on network pharmacology. *Front. Endocrinol.* **13**, 866641. https://doi.org/10.3389/fendo.2022.866641 (2022).
54. Yao, Q. et al. Osteoarthritis: pathogenic signaling pathways and therapeutic targets. *Signal. Transduct. Target. Ther.* **8**, 56. https://doi.org/10.1038/s41392-023-01330-w (2023).
55. Chan, W. C. W., Tan, Z. J., To, M. K. T. & Chan, D. Regulation and role of transcription factors in osteogenesis. *Int. J. Mol. Sci.* **22**, 5445. https://doi.org/10.3390/ijms22115445 (2021).
56. He, S. S. et al. Ferulic acid ameliorates lipopolysaccharide-induced barrier dysfunction via microRNA-200c-3p-mediated activation of PI3K/AKT pathway in Caco-2 cells. *Front. Pharmacol.* **11**, 509267. https://doi.org/10.3389/fphar.2020.00376 (2020).
57. Schnoor, M. E-cadherin is important for the maintenance of intestinal epithelial homeostasis under basal and inflammatory conditions. *Digest Dis. Sci.* **60**, 816–818. https://doi.org/10.1007/s10620-015-3622-z (2015).

Acknowledgements
The authors acknowledge the technical support of the Public Service Platform of South China Sea for R&D Marine Biomedicine Resources.

Author contributions
Writing—original draft, Luming Deng and Zhenhui Feng; investigation, Luming Deng, Lvhua Fan and Samad Tavakoli; data curation, Zhenhui Feng; methodology, Xingyan Li and Xia Wu; resources, Yuzhen Zhu; supervision, Hua Ye and Kefeng Wu; writing—review & editing, Hua Ye and Kefeng Wu; project administration, Kefeng Wu; conceptualization, Kefeng Wu; funding acquisition, Luming Deng and Kefeng Wu. All authors have read and agreed to the published version of the manuscript.

Funding
This work was supported by the Fund of Southern Marine Science and Engineering Guangdong Laboratory (Zhanjiang) (ZJW-2019-007), the Guangdong Basic and Applied Basic Research Foundation (2024A1515011074), the Science and Technology Program of Guangdong Province (2019B090905011), the Special Funds for Economic Development of Marine Economy of Guangdong Province, China (GDME-2018C011), the Special Science and Technology Innovation Project of Guangdong Province, China (2022A01207, 2019A03023), the Zhanjiang Marine Young Talent Innovation Project (2023E0007), the Administration of Traditional Chinese Medicine of Guangdong Province (20241160), and the Funds for PHD researchers of Guangdong Medical University in 2023 (GDMUB2023018).

Declarations

Competing interests
The authors declare no competing interests.

Additional information
Supplementary Information The online version contains supplementary material available at https://doi.org/10.1038/s41598-025-90011-5.

Correspondence and requests for materials should be addressed to H.Y. or K.W.